# Mini-course on Geometric Numerical Integration

David Cohen
Umeå University and University of Innsbruck
✉ david.cohen@umu.se
🌐 http://snovit.math.umu.se/~david/

February 18, 2016

## Contents

# 1 Background: Ordinary differential equations and first numerical schemes

Differential equations arise everywhere in sciences: Newton's law in physics; $N$-body problems in molecular dynamics or astronomy; population models in biology; mechanical systems in engineering; the Schrödinger equation in quantum mechanics; etc.

One can find an analytical solution to differential equations **only** in exceptional cases (with separation of variables for example), one thus **must resort to numerical simulations**!

## 1.1 Problem setting and first examples

In the first part of this lecture, we will consider the following problem

**Definition 1.1.** *Let $n \in \mathbb{N}$, $y_0 \in \mathbb{R}^n$ and $f : \mathbb{R} \times \mathbb{R}^n \to \mathbb{R}^n$ (sufficiently differentiable). One seek for a function $y := y(x) = (y_1(x), \ldots, y_n(x))^T \in \mathbb{R}^n$, $x_0 \le x \le \bar{x}$, which solves the following (system) of ordinary differential equations (ODE) (also called initial value problem (IVP))*

$$\begin{cases} y'(x) = f(x, y(x)) \\ y(x_0) = y_0. \end{cases} \tag{1}$$

*Observe that the function $f$ and the initial values $y_0$ are given.*

*In what follows, we will always assume that (1) has a unique solution $y(x)$.*

Let us look at the following examples.

**Example 1.1.** *Let us first look at a scalar differential equation and then at a system of differential equations.*

- ♦ *Scalar case ($n = 1$).* **Population dynamics**: *Let $y(t)$ be the number of individuals of a given population at time $t$.*

  *In biology, one often models the growth of a population (of bacteria for example) with the differential equation*

$$\begin{cases} y'(t) = a y(t), \\ y(0) = y_0, \end{cases}$$
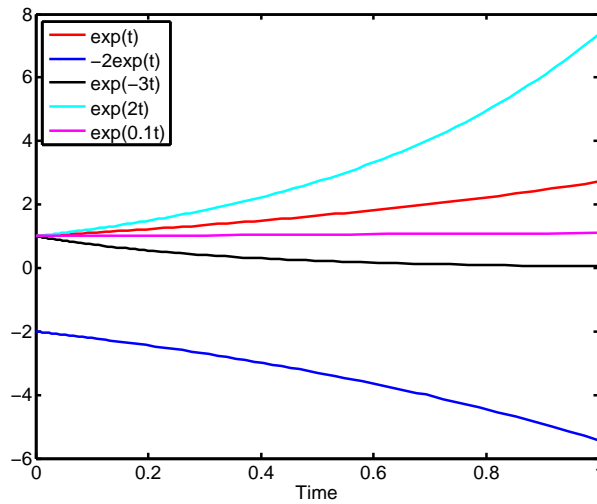
Figure 1: Exponential growth (the horizontal axis is the time).

*where the growth factor $a \in \mathbb{R}$ is given. The exact solution to the above problem reads*

$$y(t) = e^{at} y_0.$$

*In Figure 1, one can observe an exponential growth of the population (or a decrease in the case $a < 0$).*

♦ *System ($n = 2$).* **Predator-prey equations***:*

*Let*

$$\begin{aligned} y_1(t) &= \text{number of prey (for example rabbits, hares, etc.) at time } t \\ y_2(t) &= \text{number of predators (for example foxes, lynx, etc.) at time } t. \end{aligned}$$

*The dynamic of the evolution of these two populations can be described by the following differential equations ($a, b, c, d$ are given positive constants)*

$$\begin{cases} y_1' = (a - b y_2) y_1 \\ y_2' = (c y_1 - d) y_2. \end{cases}$$

*We also need the initial values $y_1(0)$ und $y_2(0)$ and the solution to our ODE is now a vector*

$$y: t \to \begin{pmatrix} y_1(t) \\ y_2(t) \end{pmatrix}.$$

*Observe that, in general, there are no explicit representation for the above solution.*

*Figure 2 shows an example taken from* `http://www.wikipedia.org`*.*

## 1.2 Euler's method

In most of the cases, it is impossible to find the exact solution $y(x)$ to our ODE (1). We will thus seek for a numerical approximation of $y(x)$ on the interval $[x_0, \bar{x}]$. For simplicity, we will consider the scalar case in this subsection.
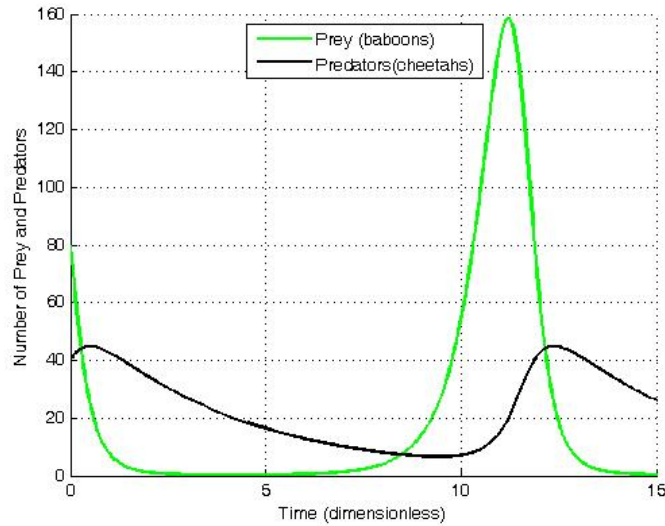
Figure 2: Progression of the two species (baboons vs cheetahs) in time (courtesy of http://www.wikipedia.org).

**Idea:** For an integer $N \geq 1$, we define the time step

$$h := \frac{\bar{x} - x_0}{N} > 0$$

and consider a partition of the interval $[x_0, \bar{x}]$ as follows

$$x_0 < x_1 < \ldots < x_N = \bar{x},$$

where

$$x_{i+1} - x_i = h \quad \text{for} \quad i = 0, 1, 2, \ldots, N.$$

For $h$ small enough, we can approximate the derivative of the exact solution at $x_0$

$$y'(x_0) = \lim_{h \to 0} \frac{y(x_0 + h) - y(x_0)}{h} \approx \frac{y(x_0 + h) - y(x_0)}{h} = \frac{y(x_0 + h) - y_0}{h}$$

and obtain (using $y'(x_0) = f(x_0, y_0)$)

$$\underbrace{y(x_1) = y(x_0 + h)}_{unknown} \approx \underbrace{y_0}_{known} + h \underbrace{f(x_0, y_0)}_{known}.$$

This is precisely the first two terms in the Taylor expansion of the exact solution $y(x)$.

A repetition of this procedure gives Euler's method (1768):

$$\boxed{y_{k+1} = y_k + h f(x_k, y_k), \quad k = 0, 1, \ldots.}$$

Here, $y_k$ is a numerical approximation of the exact solution $y(x_k)$ at $x_k$: $y_k \approx y(x_k)$ (see Figure 3).

Observe that $y_k$ depends on the time step $h$. We could thus write $y_k = y_h(x_k)$.
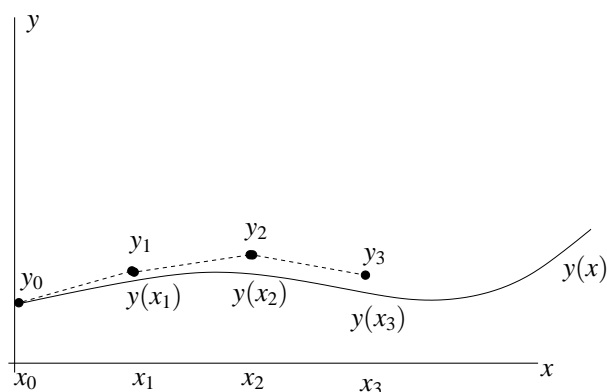
Figure 3: Euler's method.
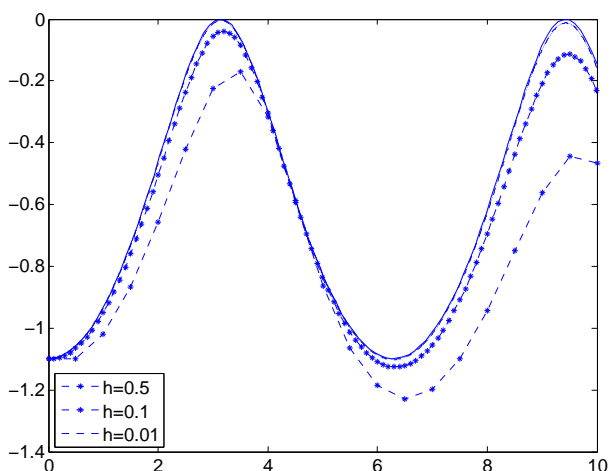


Figure 4: Euler's method with time steps $h = 0.5; 0.1; 0.01$. The straight line is the exact solution.

**Example 1.2.** *We consider the problem*

$$\begin{cases} y'(t) = e^{y(t)} \sin(t) \\ y(0) = -\ln(3). \end{cases}$$

*Figure 4 shows the exact solution, $y(t) = -\ln(\cos(x) + 2)$, and the numerical solutions obtained with Euler's method and the time steps $h = 0.5$, $h = 0.1$ and $h = 0.01$. We can observe that, the smaller $h$ is, the better the numerical approximation is!*

## 1.3   Order conditions and Runge-Kutta methods

Euler's method is an example of a <span style="color:red">one-step method</span>

$$y_{k+1} = y_k + h\phi(x_k, y_k, h),$$

by taking $\phi(x_k, y_k, h) = f(x_k, y_k)$, see above. Here, the term "one-step method" means that the numerical solution $y_{k+1}$ only depends on the earlier numerical approximation $y_k$ and not on the previous approximations $y_{k-1}, y_{k-2}$, etc.. We now define the order of a one-step method.

**Definition 1.2.** *We say that a one-step method $y_{k+1} = y_k + h\phi(x_k, y_k, h)$ has the order of convergence p, if the local error (for all nice enough problems (1)) verifies*

$$y(x_0 + h) - y_1 = \mathcal{O}(h^{p+1}), \quad h \to 0.$$

*Here, we recall that $g(h) = \mathcal{O}(h^{p+1})$, $h \to 0$ if and only if there exists a positive constant $C$ such that $|g(h)| \le Ch^{p+1}$ for all h small enough.*

Observe the following:

1. The local error is the error of the method after just **one** step. In general, and for nice enough problems, one can show that if a numerical method has order $p$, then the global error $y(x_N) - y_N$ is of the size $\mathcal{O}(h^p)$. Thus: the larger $p$ is, the more precise the numerical method is.

2. We now compute the order $p$ for Euler's method. A Taylor expansion gives

$$
\begin{aligned}
y(x_0 + h) - y_1 &= y(x_0) + \underbrace{y'(x_0)}_{=f(x_0, y_0)} h + y''(x_0)\frac{h^2}{2} + \mathcal{O}(h^3) - y_0 - hf(x_0, y_0) \\
&= \frac{y''(x_0)}{2} h^2 + \mathcal{O}(h^3) = \mathcal{O}(h^2), \quad h \to 0.
\end{aligned}
$$

Thus, the order of Euler's method is $p = 1$.

A general framework for one-step numerical methods for (1) is given by the Runge-Kutta methods.

**Definition 1.3.** *Let $s \ge 1$ be an integer, $b_i, a_{ij} \in \mathbb{R}$ for $j = 1, \ldots, i-1$ and $i = 1, \ldots, s$, $c_1 = 0$ and $c_i := \sum_{j=1}^{i-1} a_{ij}$.*

*The one-step numerical method given by*

$$
\begin{cases}
k_1 &= f(x_0, y_0) \\
k_2 &= f(x_0 + c_2 h, y_0 + h a_{21} k_1) \\
&\cdots \\
k_s &= f(x_0 + c_s h, y_0 + h \sum_{j=1}^{s-1} a_{sj} k_j) \\
y_1 &= y_0 + h \sum_{j=1}^{s} b_j k_j
\end{cases}
$$

*is called an s-stages explicit Runge-Kutta method. Here, $y_1 \approx y(h)$ using only the present value $y_0$. This one-step approximation is obtained using linear combination of the $k_j$. The quantities $k_j$ can be seen as estimated slopes of the solution to our differential equation (1), see Figure 5. The needed coefficients $a_{ij}$ and $b_j$ are usually arranged in a Butcher tableau notation:*

| $0$ | | | | |
|-----|-----|-----|-----|-----|
| $c_2$ | $a_{21}$ | | | |
| $c_3$ | $a_{31}$ | $a_{32}$ | | |
| $\vdots$ | $\vdots$ | $\vdots$ | $\ddots$ | |
| $c_s$ | $a_{s1}$ | $a_{s2}$ | $\ldots$ | $a_{s,s-1}$ |
| | $b_1$ | $b_2$ | $\ldots$ | $b_{s-1}$ | $b_s$ |

**Example 1.3.** *The tableau for Euler's method $y_1 = y_0 + hf(x_0, y_0)$ reads*

| $0$ | |
|-----|-----|
| | $1$ |

*See the homework for a further example.*
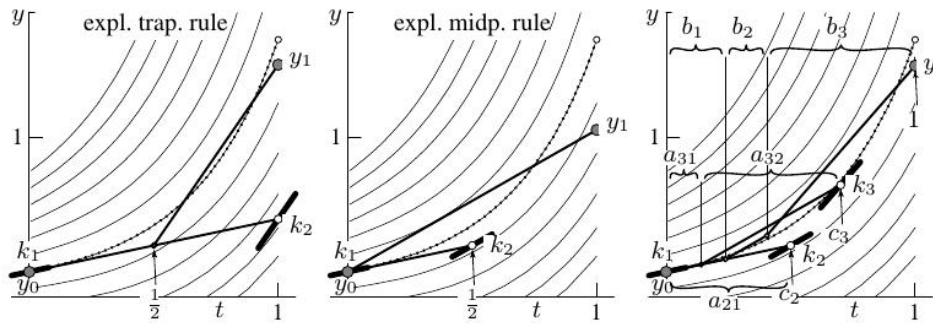
Figure 5: Various Runge-Kutta methods (courtesy of E. Hairer).

## 2   Geometric Numerical Integration: A taste

The numerical methods presented in the previous section are generic numerical schemes, they are designed to work for all generic problems (1). BUT one can develop better and more efficient numerical methods using certain **geometric structure** of a given ODE problem! In this lecture, we will focus on Hamiltonian problems in Section 3 and on highly oscillatory problems in Section 4 and the following geometric properties: preservation of the energy in Subsubsection 3.2.1; and symplecticity in Subsubsection 3.2.2; almost preservation of the oscillatory energy in Subsection 4.4.

Let us first define a few numerical methods. For ease of presentation, we will drop the explicit dependence of $x$ in the function $f$ in (1).

**Definition 2.1.** *The explicit Euler method (see above) reads*

$$y_{n+1} = y_n + h f(y_n).$$

*This simple and basic numerical method has order of convergence $p = 1$.*

**Definition 2.2.** *The implicit Euler method reads*

$$y_{n+1} = y_n + h f(y_{n+1}).$$

*Here, one has to solve a nonlinear system of equations in order to find $y_{n+1}$ (see the homework). This method has order $p = 1$.*

**Definition 2.3.** *The implicit midpoint rule reads*

$$y_{n+1} = y_n + h f\left(\frac{y_n + y_{n+1}}{2}\right).$$

*This implicit numerical method has order of convergence $p = 2$ and is symplectic (see below).*

**Definition 2.4.** *For partitioned systems (see the predator-pray model and below)*

$$\dot{u} = a(u, v)$$
$$\dot{v} = b(u, v),$$

*where $u := u(t), v := v(t)$ are independent variables and $\dot{u} := \dfrac{du}{dt}$, the partitioned Euler method reads*

$$
\begin{array}{lcl}
u_{n+1} & = & u_n + h a(u_n, v_{n+1}) \\
v_{n+1} & = & v_n + h b(u_n, v_{n+1}),
\end{array}
\quad or \quad
\begin{array}{lcl}
u_{n+1} & = & u_n + h a(u_{n+1}, v_n) \\
v_{n+1} & = & v_n + h b(u_{n+1}, v_n).
\end{array}
$$

7

*This numerical method has order $p = 1$ and is symplectic. This scheme is also called* symplectic Euler method *in connection with Hamiltonian systems, see below.*

**Definition 2.5.** *For problems of the form*

$$\dot{p} = f(q)$$
$$\dot{q} = p$$

*or $\ddot{q} = f(q)$, one defines the* Störmer-Verlet method *by*

$$q_{n+1} - 2q_n + q_{n-1} = h^2 f(q_n).$$

*In this form, this numerical method is a two-step numerical scheme and has order* 2*. Furthermore, this scheme is symplectic.*

Let us now use the above methods on the following problems.

## 2.1 Predator-Prey equations

We consider the Lotka-Volterra (or predator-prey) problem

$$\dot{u} = u \cdot (v - 2)$$
$$\dot{v} = v \cdot (1 - u).$$

This problem has the invariant

$$I(u, v) = \ln(u) - u + 2\ln(v) - v.$$

This means $I(u(t), v(t)) = Const$ for all time $t$ (see the homework). Figure 6 displays the numerical trajectories in the phase plane (periodic solutions) and monitor the above invariant along the numerical solutions given by the explicit, implicit and symplectic Euler's methods using the step size $h = 0.05$ on the time interval $[0, 24]$ and different initial values $u(0)$ and $v(0)$.

## 2.2 The mathematical pendulum

The equations of motion of a mathematical pendulum is a Hamiltonian system (discussed in more details below)

$$\dot{p} = -\sin(q)$$
$$\dot{q} = p \qquad \text{or} \quad \ddot{q} = -\sin(q)$$

and thus possess the following invariant (total energy)

$$H(p, q) = \frac{1}{2}p^2 - \cos(q).$$

Figure 7 displays the numerical trajectories (position VS time) of the pendulum and monitor the total energy along the numerical solutions given by the explicit, implicit, symplectic Euler's methods and the Störmer-Verlet scheme using the step size $h = 0.2$ on the time interval $[0, 200]$.

## 2.3 Planetary motion

We finally apply the explicit and symplectic Euler's methods to the system which describes the motion of the five outer planets relative to the sun (Figure 8). The datas are from [12, Chap. I.2.4]. This system is a (complicated) Hamiltonian problem. Figure 9 displays the numerical orbits of the planets and monitor the total energy along the numerical solutions given by the explicit and symplectic Euler's methods using the step size $h = 10$ (Earth days) on the time interval $[1994, 2268]$.
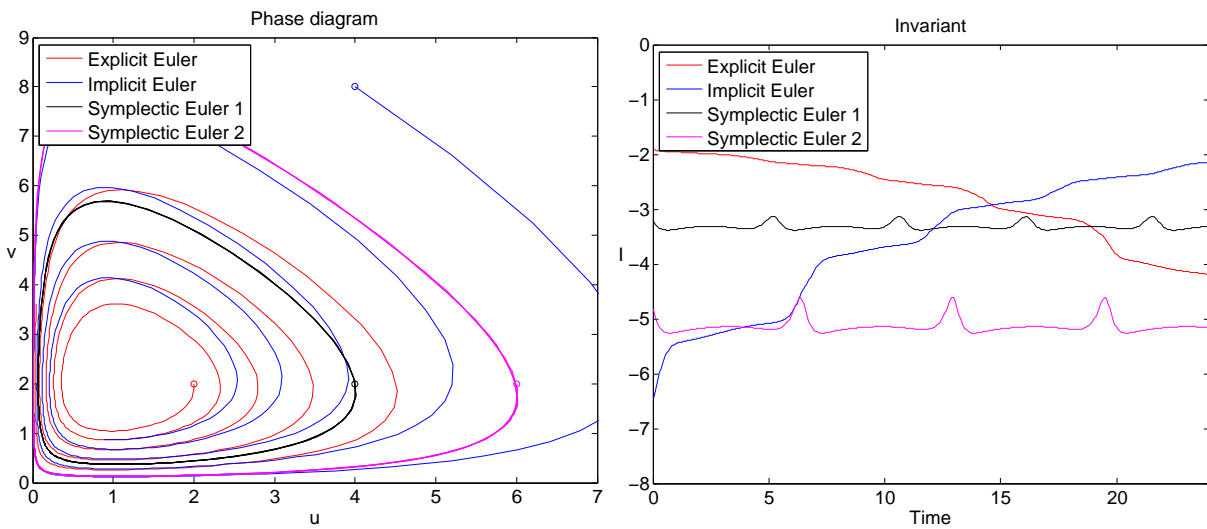
Figure 6: Numerical solutions for the Lotka-Volterra problem: Phase plane (left plot) and invariant (right plot).
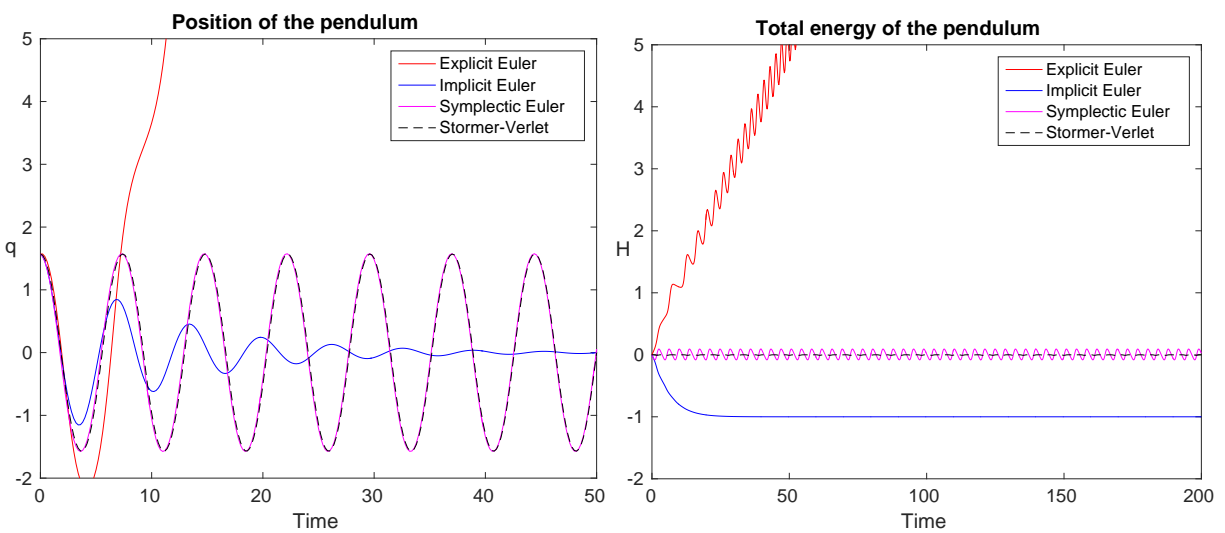


Figure 7: Numerical solutions for the mathematical pendulum: Position (left plot) and total energy (right plot).
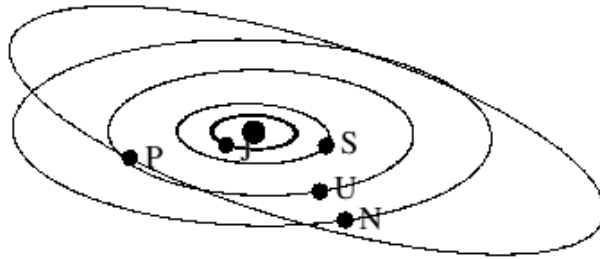
Figure 8: The outer solar system (courtesy of E. Hairer).
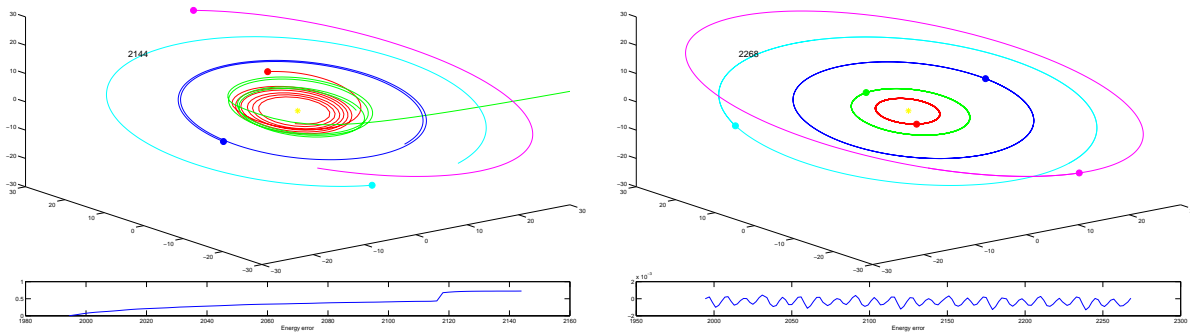


Figure 9: Numerical solutions for the outer solar system (orbits and total energy): explicit Euler (left plot) and symplectic Euler (right plot).

# 3   Numerical integration of Hamiltonian systems

Many important problems in mechanics are described by Hamiltonian systems. In this section, we will define the problem, analyse it and present some numerical schemes in order to discretise it efficiently.

## 3.1   Definition and examples

**Definition 3.1.** *Let $H : \mathbb{R}^d \times \mathbb{R}^d \to \mathbb{R}$ be given. A* Hamiltonian system *consists of the following differential equations*

$$\dot{p}_i = -\frac{\partial H}{\partial q_i}(p, q), \quad \dot{q}_i = \frac{\partial H}{\partial p_i}(p, q), \quad i = 1, \dots, d. \tag{2}$$

*Or using a more compact notation*

$$\dot{p} = -\nabla_q H(p, q) = -(\partial H / \partial q)^T, \quad \dot{q} = \nabla_p H(p, q) = (\partial H / \partial p)^T. \tag{3}$$

*Or using again another notation*

$$\dot{y} = J^{-1} \nabla H(y), \quad with \quad y = \begin{pmatrix} p \\ q \end{pmatrix} \quad and \quad J = \begin{pmatrix} 0 & I \\ -I & 0 \end{pmatrix}. \tag{4}$$

*Here, in the example of mechanical systems, one can think of the Hamiltonian H as the* **total energy** *of the problem, $q_i$ are the position coordinates and $p_i$ the momenta.*

**Example 3.1.** *The ODE for the mathematical pendulum is a Hamiltonian system. Here, the position coordinate $q(t)$ denotes the angle between the rod and the vertical at time $t$. Further, the Hamiltonian is given by $H(p, q) = \frac{1}{2} p^2 - \cos(q)$.*

*The equations describing the motion of the planets from the above section are also Hamiltonian systems. See the homework for further examples.*

## 3.2   Geometric properties of Hamiltonian systems

In this subsection, we will consider two important properties of Hamiltonian systems: conservation of the energy and symplecticity.

### 3.2.1   Conservation of the energy

We first show that the **total energy of a Hamiltonian problem** (2) **is conserved**

$$H(p(t), q(t)) = H(p(0), q(0)) \quad \text{for all time } t$$

along the exact solution of the problem. Indeed, taking the time derivative of the Hamiltonian function, one gets

$$\frac{\mathrm{d}}{\mathrm{d}t}\Big(H(p(t), q(t))\Big) = \frac{\partial H}{\partial p}\dot{p} + \frac{\partial H}{\partial q}\dot{q} = \frac{\partial H}{\partial p}\Big(-\frac{\partial H}{\partial q}\Big)^T + \frac{\partial H}{\partial q}\Big(\frac{\partial H}{\partial p}\Big)^T = 0.$$

Here, we see that the the total energy along the exact solution of a Hamiltonian system (2) is conserved. It is thus natural to develop numerical methods that share the same property as the exact solution, i. e. **energy-preserving numerical methods** (see the homework).

This is the main philosophy behind **geometric numerical integration**: derive numerical methods that share the very same geometric properties as the exact solution of a given differential equation!

### 3.2.2   Symplecticity

More important than the above property of energy conservation is the property of symplecticity of Hamiltonian systems.

Let us first consider the parallelogram $\mathscr{P} \subset \mathbb{R}^{2d}$ spanned by the vectors $\zeta = \begin{pmatrix} \zeta^p \\ \zeta^q \end{pmatrix}$ and $\eta = \begin{pmatrix} \eta^p \\ \eta^q \end{pmatrix}$ and

further the application (bilinear form)   $\omega\colon \begin{array}{ccc} \mathbb{R}^{2d} \times \mathbb{R}^{2d} & \to & \mathbb{R} \\ (\zeta, \eta) & \mapsto & \zeta^T J \eta \end{array}$   with $J = \begin{pmatrix} 0 & I \\ -I & 0 \end{pmatrix}$.

**Example 3.2.** *In the case $d = 1$, one has $\omega(\zeta, \eta) = \zeta^p \eta^q - \zeta^q \eta^p = \det \begin{pmatrix} \zeta^p & \eta^p \\ \zeta^q & \eta^q \end{pmatrix}$. This is the oriented area of the parallelogram $\mathscr{P}$!*

*In the case $d > 1$ we consider the sums of oriented areas of projections of $\mathscr{P}$ onto the coordinate plane $(p_i, q_i)$:*

$$\omega(\zeta, \eta) = \zeta^T J \eta = \sum_{i=1}^d \det \begin{pmatrix} \zeta_i^p & \eta_i^p \\ \zeta_i^q & \eta_i^q \end{pmatrix} = \sum_{i=1}^d (\zeta_i^p \eta_i^q - \zeta_i^q \eta_i^p).$$

One now asks if a map could preserve the (sum of) oriented area(s).

**Definition 3.2.** *A linear map $A\colon \mathbb{R}^{2d} \to \mathbb{R}^{2d}$ is called* symplectic *if $\omega(A\zeta, A\eta) = \omega(\zeta, \eta)$ for all $\zeta, \eta \in \mathbb{R}^{2d}$ or equivalently $A^T J A = J$.*

*Further, a differentiable map $g\colon U \subset \mathbb{R}^{2d} \to \mathbb{R}^{2d}$ is called* symplectic *if the map $g'(p, q)$ is a symplectic linear map for all $(p, q) \in U$: $g'(p, q)^T J g'(p, q) = J$ for all $(p, q) \in U$.*

Below, we will see that the solution to the Hamiltonian problem (4) is a symplectic map!

> We are thus interested in developing numerical methods which are also symplectic.

## 3.3   A few results

In this subsection, we will explain why symplectic numerical methods are well adapted to the numerical discretisation of Hamiltonian problems (4).

### 3.3.1   Characterisation of Hamiltonian problems

**Theorem 3.1** (Poincaré (1899))**.** *For every fixed time $t$, the flow $\varphi_t$ (i. e. the mapping that advances the solution by time $t$: $\varphi_t(p_0, q_0) = (p(t, p_0, q_0), q(t, p_0, q_0))$) of the Hamiltonian problem (4) is a symplectic transformation.*

This result is illustrated in Figure 10, where the level curves of the Hamiltonian function of the pendulum are displayed together with illustrations of the area preservation of the flow $\varphi_t$.

Next, we have the following result

**Theorem 3.2.** *The flow $\varphi_t$ of a differential equation $\dot{y} = f(y)$ is a symplectic transformation for all time $t$ if and only if locally $f(y) = J^{-1} \nabla H(y)$ for some function $H(y)$.*

This thus means that **symplecticity is characteristic for Hamiltonian problems**!
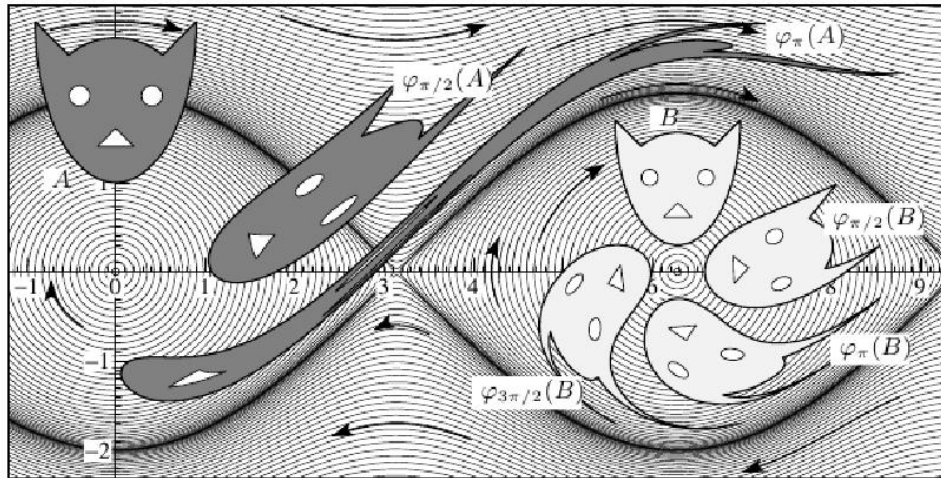
Figure 10: Area preservation of the flow of Hamiltonian systems (courtesy of E. Hairer).

### 3.3.2 Symplectic numerical methods

A numerical one-step method $y_{n+1} = \Phi_h(y_n)$ is called symplectic if, when applied to a Hamiltonian system, the discrete flow $y \mapsto \Phi_h(y)$ is a symplectic transformation for all sufficiently small step sizes $h$.
For the numerical methods we have the following results

**Theorem 3.3** (de Vogelaere (1956) and others)**.** *The symplectic Euler method defines a symplectic transformation*

$$\Phi_h : \begin{pmatrix} p_n \\ q_n \end{pmatrix} \mapsto \begin{pmatrix} p_{n+1} \\ q_{n+1} \end{pmatrix}.$$

*The same holds for the Störmer-Verlet method and the implicit midpoint rule.*

These results are illustrated in Figure 11, where one observes that the explicit Euler, the implicit Euler, and the second order Runge-Kutta methods are not symplectic, i. e. these numerical methods are not area preserving.

⚠ Ge and Marsden (1988) proved that, for Hamiltonian system without further conserved quantities, a symplectic method which exactly preserves $H$ has to be a re-parametrisation of the exact flow.

Furthermore, Chartier, Faou, Murua (2005) showed that the only symplectic method (as B-series) that conserves the Hamiltonian for arbitrary $H(y)$ is the exact flow of the differential equation. ⚠

### 3.3.3 Long-time near-energy conservation of the numerical solutions

Finally, using the idea of **backward error analysis**, one can explain the excellent long-time behaviour of symplectic methods when applied to Hamiltonian problems.

**Theorem 3.4** (Benettin, Giorgilli and others (1994))**.** *Consider the Hamiltonian system* (4) *with analytic $H$. Apply a symplectic method of order $r$ with stepsize $h$ (small enough). If the numerical solution stays in a compact set, then the numerical solution given by this symplectic scheme satisfies*

$$H(p_n, q_n) = H(p_0, q_0) + \mathcal{O}(h^r) \quad for \quad nh \le e^{\gamma/(2h)},$$
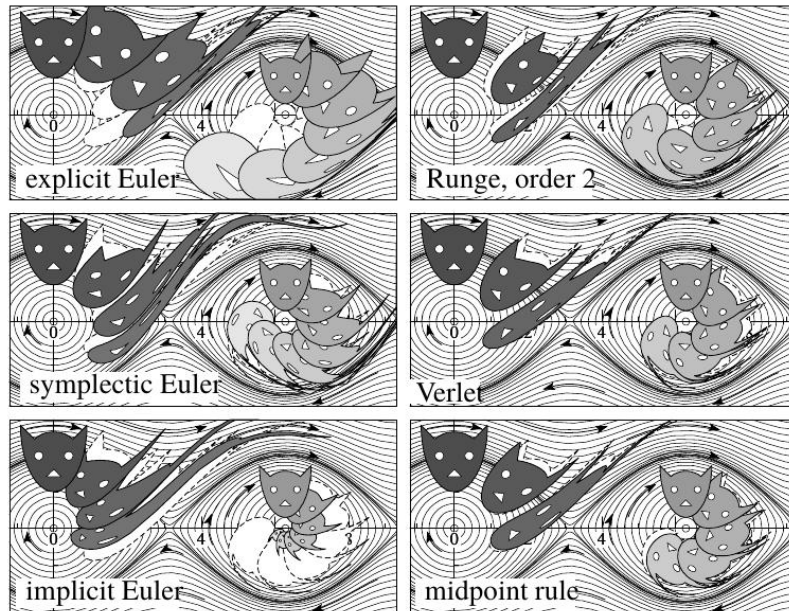
Figure 11: Area preservation of numerical methods for the pendulum (courtesy of E. Hairer).

*where $\gamma$ is a positive constant of moderate size. Recall $r = 1$ for the symplectic Euler method and $r = 2$ for the Störmer-Verlet or midpoint schemes. This explains the excellent long-time behaviour of symplectic methods when applied to Hamiltonian systems (see the plots in Figures 7 and 9 from the previous section).*

The proofs of these (nontrivial) results can be found in, for example, [12]. Let us however give the main steps for the proofs:

1. **Modified differential equation**. Consider an ODE $\dot{y} = f(y)$ together with a numerical method $y_{n+1} = \Phi_h(y_n)$. The idea of backward error analysis (BEA) is to search for a **modified differential equation** $\dot{\widetilde{y}} = f_h(\widetilde{y})$ of the form

$$\dot{\widetilde{y}} = f_h(\widetilde{y}) = f(\widetilde{y}) + h f_2(\widetilde{y}) + h^2 f_3(\widetilde{y}) + \dots,$$

such that

$$y_n \overset{!}{=} \widetilde{y}(nh)$$

and to study the difference between $f$ and $f_h$, see Figure 12.

One finds the coefficients $f_2, f_3, \dots$ of the modified differential equation using a Taylor series:

$$
\begin{aligned}
\widetilde{y}(h) = \widetilde{y}(0 + h) &= \widetilde{y}(0) + h \dot{\widetilde{y}}(0) + \frac{h^2}{2} \ddot{\widetilde{y}}(0) + \dots \\
&= y_0 + h f_h(y_0) + \dots = y_0 + h\big(f(y_0) + h f_2(y_0) + h^2 f_3(y_0) + \dots\big) + \dots \\
&\overset{!}{=} y_1 = y_0 + h f(y_0) + h^2 d_2(y_0) + h^3 d_3(y_0) + \dots \quad \text{the expansion of the numerical solution.}
\end{aligned}
$$

Observe, that the coefficients $d_j$ are given by the numerical scheme. For example, $d_j = 0$ for Euler's method.
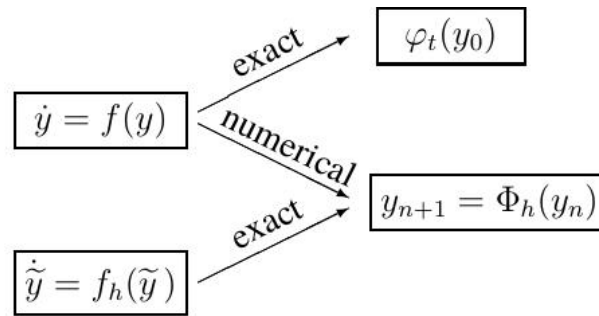
Figure 12: Modified differential equation (courtesy of E. Hairer).

One then compares the coefficients in front of $h$ and express $f_j$ thanks to the (given) coefficients of the numerical scheme $d_j$:

$$h^0: \quad y_0 = y_0$$

$$h^1: \quad f(y_0) = f(y_0)$$

$$h^2: \quad f_2(y) + \frac{1}{2}f'(y)f(y) = d_2(y)$$

$$h^3: \quad f_3(y) + \frac{1}{3!}\left(f''(f,f)(y) + f'f'f(y)\right) + \frac{1}{2}\left(f'f_2(y) + f_2'f(y)\right) = d_3(y)$$

etc.

Let us give a concrete example

**Example 3.3.** *Consider*

$$\begin{cases} \dot{y} = y^2 \\ y(0) = 1 \end{cases}$$

*with exact solution* $y(t) = \frac{1}{1-t}$. *The modified differential equation for explicit Euler's method reads*

$$\dot{\tilde{y}} = f_h(\tilde{y}) = \tilde{y}^2 - h\tilde{y}^3 + \frac{h^2}{2}3\tilde{y}^4 - \frac{h^3}{3}8\tilde{y}^5 \pm \dots$$

*and the exact solution of the modified differential equation* $\dot{\tilde{y}} = f_h(\tilde{y})$ *is the numerical solution given by Euler's method!*

2. **Properties of the modified differential equation**.

   If the numerical methods has order $p$, then the modified equation reads $\dot{\tilde{y}} = f(\tilde{y}) + h^p f_{p+1}(\tilde{y}) + \dots$.

   If the original problem is Hamiltonian and the numerical method is symplectic, then the modified equation is also Hamiltonian!

3. **Some estimations**. Using the analyticity of the function $f$ and further technical assumptions, one next estimates the coefficients $d_j(y)$ and the coefficients $f_j(y)$ of the modified differential equation. One has to truncate the modified equation at an appropriate index $N$ and obtain an estimate for the local error

$$\|\Phi_h(y_0) - \varphi_{N,h}(y_0)\| \le Ce^{-h^*/h} \quad \text{for} \quad h \le h^*,$$

where $\varphi_{N,h}(y_0)$ is the exact solution of the truncated modified differential equation

$$\dot{\tilde{y}} = f(\tilde{y}) + h f_2(\tilde{y}) + \ldots + h^{N-1} f_N(\tilde{y})$$

and $\Phi_h(y_0)$ is our numerical method.

4. **Near conservation of the total energy**. Consider a Hamiltonian problem with a symplectic numerical method of order $p$. We know that the modified equation is Hamiltonian with

$$\widetilde{H}(y) = H(y) + h H_2(y) + h^2 H_3(y) + \ldots + h^{N-1} H_N(y).$$

For small enough step sizes $h$ and an appropriate truncation index $N$, one can show that

$$\widetilde{H}(y_n) = \widetilde{H}(y_0) + \mathcal{O}(e^{-h^*/(2h)})$$

and prove near conservation of the energy by a symplectic numerical method of order $p$:

$$H(y_n) = H(y_0) + \mathcal{O}(h^p)$$

for exponential long time $nh \le T = e^{h^*/(2h)}$!

# 4 Highly oscillatory problems

This section deals with the numerical treatment of particular second-order differential equations with highly oscillatory solutions.

## 4.1 Motivation: A Fermi-Pasta-Ulam type problem

We consider

$$\ddot{x} + \Omega^2 x = g(x) := -\nabla U(x),$$
$$x(0) = \tilde{x}, \dot{x}(0) = \dot{\tilde{x}}, \tag{5}$$

where

$$\Omega = \begin{pmatrix} 0 & 0 \\ 0 & \omega I \end{pmatrix}$$

with $\omega \gg 1$, $x := (x_{\text{slow}}, x_{\text{fast}}) = (x_0, x_1) \in \mathbb{R}^{n \times m}$, the nonlinearity $g$ comes from a smooth potential $U$, and we assume finite initial energy

$$\frac{1}{2} \|\dot{x}(0)\|^2 + \frac{1}{2} \|\Omega x(0)\|^2 \le E. \tag{6}$$

We want to use a numerical method with large step size, so that the product $h \cdot \omega$ is **not** small and thus the BEA from the previous section **cannot** be applied in this situation!

A typical model problem is offered by the (modified) Fermi-Pasta-Ulam problem (FPU).

**Example 4.1.** *The FPU problem consists of a chain of alternating stiff (linear) and soft (nonlinear) springs as described in Figure 13.*

*After a change of coordinates, one gets the Hamiltonian*

$$H(x, y) = \frac{1}{2} y^T y + \frac{1}{2} x^T \Omega^2 x + U(x)$$

*which gives a differential equation of the form* (5).
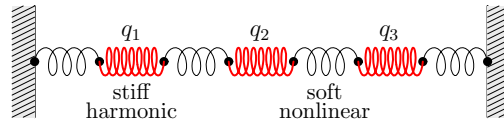
Figure 13: FPU problem (courtesy of E. Hairer).
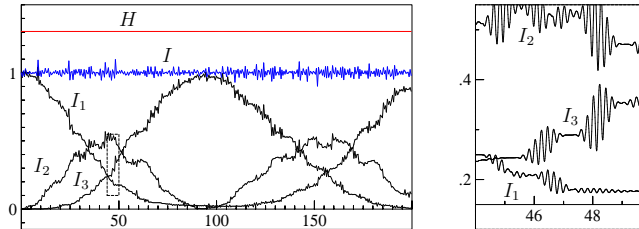


Figure 14: Energy exchange in the FPU problem ($H$=total energy, $I_1, I_2, I_3$ components of the oscillatory energy $I$).

*Denoting the energy of the $j$-the stiff spring by*

$$I_j(x_{1,j}, y_{1,j}) := \frac{1}{2}(y_{1,j}^2 + \omega^2 x_{1,j}^2),$$

*we observe, in Figure 14, that the <span style="color:red">oscillatory energy</span>*

$$I(x, y) := I_1 + I_2 + \ldots + I_m$$

*remains almost constant for very long time along the exact solution of the FPU problem!*

*We want to understand this phenomena. An explanation will be given in the two sections.*

*Let us investigate what happen for the numerical solutions given by classical methods. To do so, we consider the above FPU problem with $\omega = 50$ and $3$ stiff springs. In Figure 15, one can observe that the classical numerical schemes (implicit midpoint rule, classical RK4, Störmer-Verlet) do not perform well or ar not very efficient (the midpoint rule needs the solution to a nonlinear system at each time step)!*

*How do we get better numerical integrators for highly oscillatory problems?*

*The next subsections will provide an answer to this question.*

## 4.2   Trigonometric integrators

We now present efficient numerical methods for highly oscillatory problems of the form (5) having the following properties:
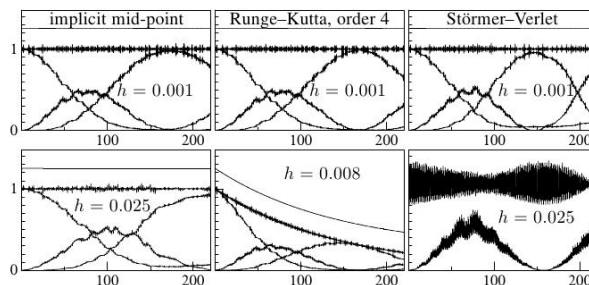


Figure 15: FPU problem: Numerical solutions for various integrators (courtesy of E. Hairer).

1. they reduce to the Störmer-Verlet scheme if $\Omega = 0$

2. they are exact if $g \equiv 0$

3. they work well for $h\omega \geq c_0 > 0$

4. they are explicit

5. they almost preserve $H$ and $I$ for very long time.

The main building block for the derivation of these scheme is the variation of constants formula for the exact solution ($h$ is a positive real number)

$$x(h) = \cos(h\Omega)x(0) + \Omega^{-1}\sin(h\Omega)\dot{x}(0) + \int_0^h \Omega^{-1}\sin((h-s)\Omega)g(x(s))\,\mathrm{d}s$$

$$\dot{x}(h) = -\Omega\sin(h\Omega)x(0) + \cos(h\Omega)\dot{x}(0) + \int_0^h \cos((h-s)\Omega)g(x(s))\,\mathrm{d}s.$$

Discretising the above integrals (in various ways) motivates the following definition

**Definition 4.1.** *The family of* trigonometric methods *reads*

$$x_{n+1} = \cos(h\Omega)x_n + \Omega^{-1}\sin(h\Omega)\dot{x}_n + \frac{1}{2}h^2\Psi g_n \tag{7}$$

$$\dot{x}_{n+1} = -\Omega\sin(h\Omega)x_n + \cos(h\Omega)\dot{x}_n + \frac{1}{2}h(\Psi_0 g_n + \Psi_1 g_{n+1}), \tag{8}$$

*where* $g_n := g(\Phi x_n)$, $\Phi = \Phi(h\Omega)$, $\Psi = \Psi(h\Omega)$, $\Psi_1 = \Psi_1(h\Omega)$, $\Psi_2 = \Psi_2(h\Omega)$ *are* filter functions. *The purpose of these filter functions is to filter out numerical resonances and the choice of these filter functions is not an easy task. Let us give two examples.*

**Example 4.2.** *The choices* $\Psi(\zeta) = \mathrm{sinc}(\zeta) := \frac{\sin(\zeta)}{\zeta}, \Phi(\zeta) = 1, \Psi_0(\zeta) = \cos(\zeta), \Psi_1(\zeta) = 1$ *was proposed by Deuflhard in* 1979.

*The choices* $\Psi(\zeta) = \mathrm{sinc}^3(\zeta), \Phi(\zeta) = \mathrm{sinc}(\zeta), \Psi_0(\zeta) = \cos(\zeta)\mathrm{sinc}^2(\zeta), \Psi_1(\zeta) = \mathrm{sinc}^2(\zeta)$ *was proposed by Grimm and Hochbruck in* 2006.

## 4.3 Modulated Fourier expansions

In order to show near-conservation of the oscillatory energy along the exact solution and the near-conservation of the oscillatory and total energy along the numerical solutions given by the trigonometric integrators, we make use of an analytical tool called a modulated Fourier expansion. We present this tool now.

To motivate a suitable ansatz for the exact solution of (5), we observe that the general solution of the scalar problem $\ddot{x} + \omega^2 x = g(t)$ is given by

$$x_{\mathrm{gen}} = x_{\mathrm{part}} + x_H,$$

where $x_H = d_1\mathrm{e}^{\mathrm{i}\omega t} + d_2\mathrm{e}^{-\mathrm{i}\omega t}$ and $x_{\mathrm{part}} = c_0(t) + \omega^{-1}c_1(t) + \omega^{-2}c_2(t) + \ldots$. Thus

$$x(t) = x_{\mathrm{part}}(t) + x_H(t) =: y(t) + \mathrm{e}^{\mathrm{i}\omega t}z(t) + \mathrm{e}^{-\mathrm{i}\omega t}\bar{z}(t)$$

with smooth functions $y$ (real) and $z$ (complex), i.e. these functions and their derivatives are bounded independently of $\omega \gg 1$.

If $g$ now depends on $x$, one needs to consider more and more terms of the form $\mathrm{e}^{\mathrm{i}k\omega t}z^k(t)$, for integers $k$, in order to describe the solution.

This motivates the following result presenting a modulated Fourier expansion (MFE) for the exact solution to highly oscillatory problems:

**Theorem 4.1** (Hairer, Lubich (2000))**.** *Let $x(t)$ be the solution to* (5) *with initial data satisfying* (6)*. Assume that $x(t)$ stays in a compact $K$ for $0 \le t \le T$. Then, one has*

$$x(t) = y(t) + \sum_{0 < |k| < N} \mathrm{e}^{\mathrm{i}k\omega t} z^k(t) + R_N(t) \tag{9}$$

*for arbitrary $N \ge 2$. Moreover, $R_N(t) = \mathcal{O}(\omega^{-N-2})$, $y_0 = \mathcal{O}(1)$, $y_1 = \mathcal{O}(\omega^{-2})$, $z_0^1 = \mathcal{O}(\omega^{-3})$, $z_1^1 = \mathcal{O}(\omega^{-1})$, $z^k = \mathcal{O}(\omega^{-k-2})$ and $z^{-k} = \overline{z^k}$ for all $k$.*

This analytical tool permits to show that the oscillatory energy $I$ is almost preserved for very long time along the exact solution to (5).

**Theorem 4.2** (Hairer, Lubich (2000))**.** *Under the assumptions of the above theorem and assuming further that the solution $x(t)$ to* (5) *stays in a compact for $0 \le t \le \omega^N$, then one has*

$$I(x(t), \dot{x}(t)) = I(x(0), \dot{x}(0)) + \mathcal{O}(\omega^{-1}) + \mathcal{O}(t\omega^{-N}),$$

*where the constant in $\mathcal{O}(\cdot)$ depends on $E, N$ but is independent of $\omega$ and $t$ with $0 \le t \le \omega^N$.*

Furthermore, near-conservation of $I$ over exponentially long time intervals is shown in Cohen, Hairer, Lubich (2000).

## 4.4   Long-time behaviour of the numerical solutions

As for the analytical solution, one can find a MFE

$$x_h(t) = \sum_{|k| < N} \mathrm{e}^{\mathrm{i}k\omega t} z_h^k(t)$$

for the numerical solution given by the trigonometric method (7) by requiring that

$$x_n \overset{!}{=} x_h(nh).$$

Under some technical assumptions, one finally obtains a result on long-time near-conservation properties for the trigonometric methods

**Theorem 4.3** (Hairer, Lubich (2000))**.** *The numerical solution given by the trigonometric methods* (7) *satisfies, for $0 \le nh \le h^{-N-1}$,*

$$H(x_n, \dot{x}_n) = H(x_0, \dot{x}_0) + \mathcal{O}(h)$$
$$I(x_n, \dot{x}_n) = I(x_0, \dot{x}_0) + \mathcal{O}(h).$$

*The constants symbolised by $\mathcal{O}(\cdot)$ are independent of $n, h, \omega$ but depend on $N$.*

This theorem explains the excellent long-time behaviour of the trigonometric methods when applied to highly oscillatory problems.

# 5   GNI for PDEs and S(P)DEs

In this section, we briefly review some results dealing with geometric numerical methods for **partial differential equations** (PDEs) and **stochastic (partial) differential equations** (S(P)DEs). These are active ongoing research areas and we therefor try to keep the exposition without too much technical details.

## 5.1  Long-time numerical integration of wave equations

The goal of this subsection is to illustrate the use of geometric numerical integration in the simulation of evolution equations possessing geometric properties over long times. Of particular interest are Hamiltonian partial differential equations typically arising in wave propagation phenomena or quantum mechanics. We refer to [6] or [5] for a detailed exposition on the subject.

Extending the modulated Fourier expansion from the previous section, one obtains interesting results on the long-time behaviour of nonlinear wave equations and their numerical discretisation. In particular, we will show long-time near conservation of the energy, the momentum and the actions along numerical discretisations of semi-linear wave equations.

The presentation of this subsection is inspired by materials from E. Hairer and Ch. Lubich.

### 5.1.1  Semi-linear wave equations

We consider the one-dimensional semi-linear wave equation

$$u_{tt} - u_{xx} + \rho u + g(u) = 0, \tag{10}$$

where $u = u(x, t)$ for $t > 0$ and $-\pi < x < \pi$ with periodic boundary conditions. We assume $\rho > 0$ and $g$ smooth with $g(0) = g'(0) = 0$.

The above equation reads, in terms of the Fourier series (obs. $u_{-j} = \overline{u}_j$) $u(x, t) = \sum_{j=-\infty}^{\infty} u_j(t) e^{\mathrm{i}jx}$,

$$\ddot{u}_j + \omega_j^2 u_j = -\mathscr{F}_j g(u) \quad \text{for} \quad j \in \mathbb{Z}, \tag{11}$$

with the frequencies $\omega_j = \sqrt{j^2 + \rho}$ and $u_j = \mathscr{F}_j u$ denotes the Fourier coefficients. This motivates the use of trigonometric methods for the time discretisation of semi-linear wave equations (see below).

The following quantities are exactly conserved along every solution $(u(x, t), v(x, t))$, where $v := u_t$, of the semi-linear wave equation (10) (here one has $U'(u) = g(u)$):

$$\text{Total energy or Hamiltonian} \quad H(u, v) = \frac{1}{2\pi} \int_{-\pi}^{\pi} \left( \frac{1}{2} \left( v^2 + (u_x)^2 + \rho u^2 \right)(x) + U(u(x)) \right) \mathrm{d}x$$

$$\text{Momentum} \quad K(u, v) = \frac{1}{2\pi} \int_{-\pi}^{\pi} u_x(x) v(x) \, \mathrm{d}x = - \sum_{j=-\infty}^{\infty} \mathrm{i}j u_{-j} v_j.$$

Furthermore, it can be shown (see below) that the harmonic actions

$$I_j(u, v) = \frac{1}{2} \left( \omega_j |u_j|^2 + \frac{1}{\omega_j} |v_j|^2 \right) \quad \text{for} \quad j \in \mathbb{Z} \tag{12}$$

remain constant up to small deviations over long times for almost all values of $\rho > 0$, when the initial data are smooth and small enough (Bambusi (normal forms), Bourgain, or Cohen, Hairer, Lubich (MFE)). This is illustrated in Figure 16, where one plots the actions for the solution of the semi-linear wave equation $u_{tt} - u_{xx} + u = u^2$ with initial values $u(x, 0) = \varepsilon(1 - \frac{x^2}{\pi^2})^2$ and $v(x, 0) = 0$ for $\varepsilon = 0.5$.

We now make this statement more precise. For $s \geq 0$, we work with the Sobolev space on the torus $\mathbb{T}$

$$H^s = \left\{ v \in L^2(\mathbb{T}) : \|v\| < \infty \right\} \quad \text{with weighted norm} \quad \|v\|_s = \left( \sum_{j=-\infty}^{\infty} \omega_j^{2s} |v_j|^2 \right)^{1/2}.$$

We further assume that the initial position and velocity of (10) satisfy

$$\|u(\cdot, 0)\|_{s+1}^2 + \|v(\cdot, 0)\|_s^2 \leq \varepsilon^2$$

for suitably large $s$ and small $\varepsilon$. We then get the result
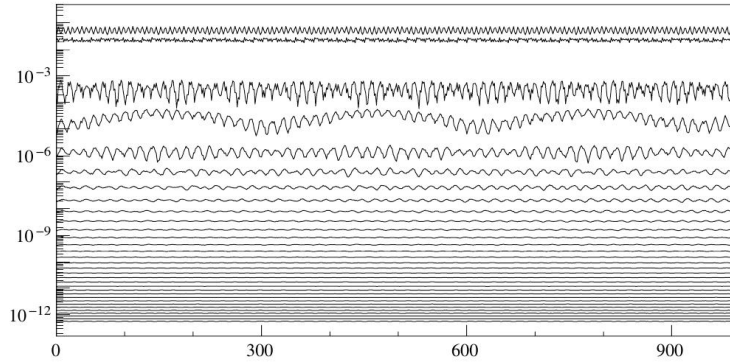
Figure 16: Near-conservation of actions: the first 32 actions $I_j(t)$ are plotted as functions of time.

**Theorem 5.1** (Cohen, Hairer, Lubich (2008)). *Under suitable non-resonance condition on the frequencies $\omega_j$, the above assumption on the initial values, the estimate*

$$\sum_{\ell=0}^{\infty} \omega_\ell^{2s+1} \frac{I_\ell(t) - I_\ell(0)}{\varepsilon^2} \leq C\varepsilon \quad for \quad 0 \leq t \leq \varepsilon^{-N},$$

*with $I_\ell(t) := I_\ell(u(\cdot,t), v(\cdot,t))$ holds with a constant C which depends on s and N, but is independent of $\varepsilon$ and t.*

*This implies long-time regularity of the exact solution to* (10)

$$\|u(\cdot,t)\|_{s+1}^2 + \|v(\cdot,t)\|_s^2 \leq 2\left(\|u(\cdot,0)\|_{s+1}^2 + \|v(\cdot,0)\|_s^2\right) \quad for \quad t \leq \varepsilon^{-N}.$$

*This, more or less, says that if one starts small, one remains small for very long time.*

The main tool used for the proofs of the above results is a modulated Fourier expansion of the exact solution to the semi-linear wave equation (10).

### 5.1.2   Numerical discretisation of semi-linear wave equations

For the numerical discretisation of (10), we first discretise in space (pseudo-spectral discretisation) and then in time (trigonometric method).

The real-valued trigonometric polynomial (where the prime indicates that the first and last terms in the sum are taken with factor 1/2)

$$u^M(x,t) = \sum_{|j| \leq M}' q_j(t) e^{ijx}$$

is chosen such that the wave equation (10) is fulfilled at the $2M$ equidistant collocation points $x_k := k\pi/M$ for $k = -M, \ldots, M-1$. This gives the **system of ODE** for $q = (q_j)_{j=-M}^{M-1}$ (obs. the analogy with the highly oscillatory problem studied in Section 4):

$$\frac{d^2 q}{dt^2} + \Omega^2 q = f(q) \quad with \quad f(q) = -\mathscr{F}_{2M} g(\mathscr{F}_{2M}^{-1} q).$$

Here, the matrix $\Omega = \text{diag}(\omega_j)_{j=-M}^{M-1}$ is diagonal and $\mathscr{F}_{2M}$ denotes the discrete Fourier transform

$$(\mathscr{F}_{2M} w)_j = \frac{1}{2M} \sum_{k=-M}^{M-1} w_k e^{-ijx_k}.$$
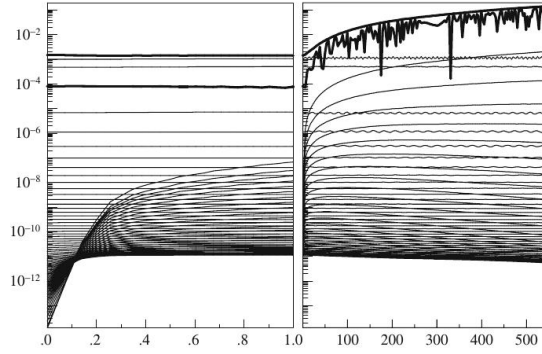
Figure 17: Actions, total energy (upper bold line), and momentum (lower bold line) along the numerical solution of DOPRI5 for the CFL number $h\omega_M \approx 1.075$.

For the above system, one can define a discrete Hamiltonian $H_M(p,q)$, a discrete momentum $K_M(p,q)$ and discrete actions $E_j(p,q)$ for $|j| \le M$ and $p = \dot{q}$.

Using a modulated Fourier expansions for the numerical solution, one can then prove

**Theorem 5.2** (Cohen, Hairer, Lubich (2008)). *Assume a non-resonance conditions for the frequencies $\omega_j$ and initial values that are smooth and small in a Sobolev norm of sufficiently high order $s$. The numerical solution given by a pseudo-spectral discretisation of* (10) *in space and a time discretisation by symplectic trigonometric method satisfies*

$$\frac{H_M(p_n, q_n) - H_M(p_0, q_0)}{\varepsilon^2} \le C\varepsilon$$

$$\frac{K_M(p_n, q_n) - K_M(p_0, q_0)}{\varepsilon^2} \le C(\varepsilon + M^{-s} + \varepsilon t M^{-s+1})$$

$$\sum_{\ell=0}^{M} \omega_\ell^{2s} \frac{E_\ell(p_n, q_n) - E_\ell(p_0, q_0)}{\varepsilon^2} \le C\varepsilon$$

*for long times $t = nh \le \varepsilon^{-N}$ with a constant $C$ that is independent of the small parameter $\varepsilon$, the dimension $2M$ of the spatial discretisation, the time stepsize $h$ and the time $t = nh \le \varepsilon^{-N}$.*

The above result is illustrated in Figures 17 and 18. The same equation as above is discretised in time first by an explicit adaptive Runge-Kutta scheme (Figure 17) and then by a trigonometric method (Figure 18).

The main steps for the proof of the above theorem are:

1. Write a MFE for the numerical solution

$$\tilde{q}_h(t) = \sum_{\mathbf{k}} e^{i(\mathbf{k}\cdot\omega)\mathbf{t}} z^{\mathbf{k}}(\varepsilon t).$$

   The sum is over all $\mathbf{k} = (k_\ell)_{\ell \ge 0}$.

2. Prove existence of smooth functions $z^{\mathbf{k}}(\tau)$ with derivatives bounded independently of $\varepsilon$ (on intervals of length $\varepsilon^{-1}$).
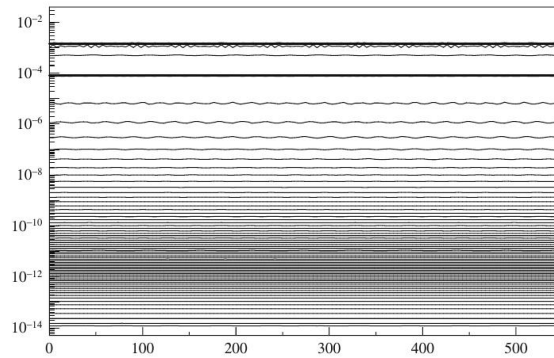
Figure 18: Actions, total energy (upper bold line), and momentum (lower bold line) along the numerical solution of the trigonometric integrator for the CFL number $h\omega_M \approx 6.4$.

3. Establish a Hamiltonian structure and the existence of formal invariants in the differential and algebraic equations for the functions $z^{\mathbf{k}}(\tau)$.

4. Prove closeness (on intervals of length $\varepsilon^{-1}$) of the formal invariants to actions $E_\ell$, to the total energy $H_M$, and to the momentum $K_M$.

5. Stretch from short to long intervals of length $\varepsilon^{-N+1}$ by patching together previous results along an invariant.

### 5.1.3  Further results in the subject

Using the techniques of modulated Fourier expansions, one can prove the following results

1. Long-time near-conservation of energy, actions, momentum for the Störmer-Verlet/leapfrog discretisation of the semi-linear wave equation (using stepsizes in the linear stability interval).

2. Long-time stability of plane wave solutions of the cubic Schrödinger equation (cubic NLS) (Faou, Gauckler, Lubich (2013)).

3. Long-time stability of plane waves of the cubic NLS for the numerical discretisation by Fourier collocation and Strang splitting (Faou, Gauckler, Lubich (2013)).

4. Long-time near-conservation of actions, energy, and momentum along numerical solutions of the cubic NLS (pseudo-spectral and Lie-Trotter splitting) (Gauckler, Lubich (2010)).

5. Long-time near-conservation of actions, energy, mass, and momentum along numerical solutions of the cubic NLS (pseudo-spectral and exponential integrators) (Cohen, Gauckler (2012)).

## 5.2  Stochastic geometric numerical integration

The last decade has seen a growing interest in the development and numerical analysis of geometric numerical integrators for stochastic (partial) differential equations (S(P)DEs). We now review some results on the subject. These result are connected to the above material.

But first, some background materials.
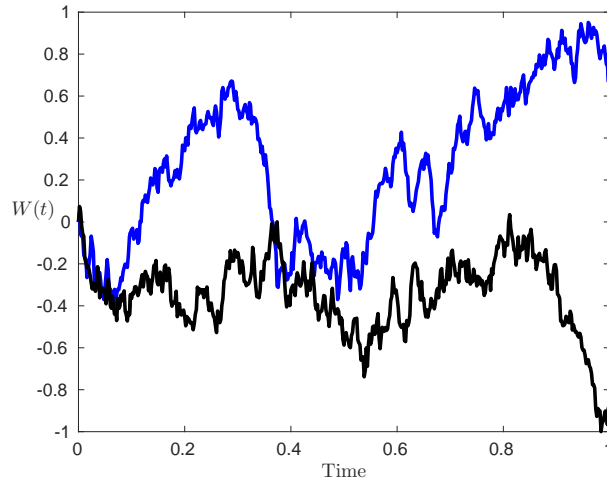
Figure 19: 2 realisations of a Brownian motion on $[0,1]$.

### 5.2.1  Stochastic differential equations and Euler-Maruyama scheme

Let us consider two (scalar, for simplicity) functions $f$ and $g$ and a real (for simplicity) initial value $X_0$. A scalar stochastic differential equation (SDE) on the time interval $[0,T]$ reads:

$$\mathrm{d}X(t) = f(X(t))\,\mathrm{d}t + g(X(t))\,\mathrm{d}W(t)$$
$$X(0) = X_0 \tag{13}$$

or in the equivalent integral form

$$X(t) = X_0 + \int_0^t f(X(s))\,\mathrm{d}s + \int_0^t g(X(s))\,\mathrm{d}W(s), \quad 0 \le t \le T. \tag{14}$$

Here the second integral on the right-hand side is to be taken with respect to a scalar standard Brownian motion, also called, standard Wiener process $W(t)$, see Figure 19.

This object is a random variable that depends continuously on $t \in [0,T]$ and satisfies the following conditions:

(W1)  $W(0) = 0$ with probability one.

(W2)  For $0 \le s < t \le T$, the increment $W(t) - W(s)$ is normally distributed with mean zero and variance $t - s$. We thus have $W(t) - W(s) \sim \sqrt{t-s}\,N(0,1)$. Here $N(0,1)$ denotes the standard normal distribution (or Gaussian) with mean zero and variance one.

(W3)  For $0 \le s < t < u < v \le T$, the increments $W(t) - W(s)$ and $W(v) - W(u)$ are independent.

The classical Euler method for ODEs can be adapted to the case of the SDE (13) and reads

$$X_{n+1} = X_n + f(X_n)h + g(X_n)\Delta W_n, \tag{15}$$

where $h$ denotes the step size and $\Delta W_n := W_{n+1} - W_n := W(t_{n+1}) - W(t_n) \sim \sqrt{h}\,N(0,1)$ are Wiener increments. The Euler-Maruyama scheme thus provides numerical approximations $X_n \approx X(t_n)$ at the discrete times $t_n = nh$.

Classical references on the numerical integration of SDEs are [14, 18, 22, 21].

### 5.2.2   Long-time integration of stochastic oscillators

Stochastic versions of the Hamiltonian problems considered in the previous sections have been investigated recently together with their numerical discretisations by stochastic symplectic schemes. We refer to [22] and references therein.

Instead, we shall focus of the long-time numerical discretisation of (scalar) stochastic oscillators of the form [24]

$$\ddot{x}(t) + \omega^2 x(t) = \alpha \dot{W}(t),$$

or written as a second-order SDE

$$dX(t) = Y(t)\,dt$$
$$dY(t) = -\omega^2 X(t)\,dt + \alpha\,dW(t), \tag{16}$$

where $W(t)$ is the scalar Wiener process defined above, the parameters $\omega \gg 1$ and $\alpha \in \mathbb{R}$, and we denote by $X_0$ and $Y_0$ the initial values.

The unique solution to (16) reads (variation-of-constants formula)

$$X(t) = X_0 \cos(\omega t) + Y_0 \omega^{-1} \sin(\omega t) + \alpha \int_0^t \omega^{-1} \sin(\omega(t-s))\,dW(s),$$

$$Y(t) = -X_0 \omega \sin(\omega t) + Y_0 \cos(\omega t) + \alpha \int_0^t \cos(\omega(t-s))\,dW(s) \tag{17}$$

and verifies

$$\mathbb{E}\left[\frac{1}{2}\big(Y(t)^2 + \omega^2 X(t)^2\big)\right] = \frac{1}{2}\big(Y_0^2 + \omega^2 X_0^2\big) + \frac{\alpha^2}{2} t \quad \text{for all time} \quad t. \tag{18}$$

This corresponds to the fact that the expectation of the total energy of (16) drifts linearly with time.

Since we are interested in the long-time behaviour of the numerical solutions, the model problem (16) with the above property will serve as a test in order to derive efficient numerical methods!

Numerical discretisation of this problem was recently investigated by: Strømmen Melbø, Higham, Cohen, Sigg, Tocino, Senosiain, Hong, Scherer, Wang, de la Cruz, etc. Some of the obtained results are

1. Euler-Maruyama: exponential growth of the expected energy;

2. Backward Euler-Maruyama: slower growth rate;

3. Midpoint rule: asymptotically correct growth rate;

4. Stochastic $\theta$-method: wrong growth rate;

5. Stochastic trigonometric method: exact growth rate;

6. Predictor-corrector methods: asymptotically correct growth rate.

The long-time behaviour of some of the above numerical methods is illustrated in Figure 20. To produce this figure, we use $\omega = 5$, $X_0 = 0$, $Y_0 = 1$, $\alpha = 1$ and consider the Euler-Maruyama (EM), the partitioned EM (pEM), the backward EM (BEM) and the stochastic trigonometric method (STM) with (large) stepsize $h = 0.2$. The STM is the only numerical method offering a proper behaviour with respect to the drift of the expected energy. Observe that the numerical solution given by EM cannot be seen in this figure since it blows up very rapidly.
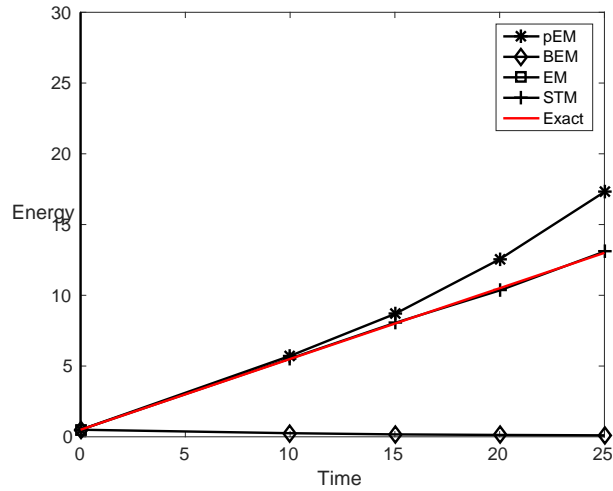
Figure 20: Stochastic oscillator: Linear growth in the energy for various numerical solutions.

### 5.2.3 Long-time integration of linear stochastic wave and stochastic Schrödinger equations

As also seen in the deterministic setting, the test equation (16) can serve as a model problem for more complicated ones such as linear stochastic wave equations and stochastic Schrödinger equations. Indeed, a (pseudo-spectral) spatial discretisation of such SPDEs leads to a system of SDEs of the form (16).

Without going into too much technical details, one can extend the stochastic trigonometric method (STM) to the time discretisation of the linear stochastic wave equation

$$
\begin{aligned}
&\mathrm{d}\dot{u} - \Delta u \, \mathrm{d}t = \mathrm{d}W && \text{in } \mathscr{D} \times (0, \infty), \\
&u = 0 && \text{in } \partial\mathscr{D} \times (0, \infty), \\
&u(\cdot, 0) = u_0, \ \dot{u}(\cdot, 0) = v_0 && \text{in } \mathscr{D},
\end{aligned}
$$

where the stochastic process $\{W(t)\}_{t \geq 0}$ is an $L_2(\mathscr{D})$-valued $Q$-Wiener process. One can show that the exact solution to this problem as well as the numerical solution given by the STM have the very same drift in the expected energy, see [4] for details and Figure 21 for an illustration. To produce this figure, we discretise the above SPDE in space by FEM with mesh $h = 0.1$ and the following numerical methods are used for the time discretisation: the stochastic trigonometric method (STM), the backward Euler-Maruyama (BEM), the stochastic Störmer-Verlet (SV), the Crank-Nicolson-Maruyama (CNM) with time step $k = 0.1$. In this figure, one clearly observes that the only scheme preserving the linear drift of the expected energy $\mathbb{E}[\|\Delta^{1/2} u_1(t)\|^2_{L_2} + \|u_2(t)\|^2_{L_2}]$ is the stochastic trigonometric method. Here we denote $u_1 := u$ and $u_2 := \dot{u}$.

Finally, long-time behaviour of the exact and numerical solution were also investigated in the context of the linear stochastic Schrödinger equation

$$
\begin{aligned}
&\mathrm{i}\mathrm{d}u - \Delta u \, \mathrm{d}t = \mathrm{d}W && \text{in } \mathbb{R}^d \times (0, \infty), \\
&u(0) = u_0 && \text{in } \mathbb{R}^d.
\end{aligned}
$$

Once again, it can be shown that the stochastic exponential method outperforms classical numerical schemes in term of the long-time behaviour of the expected mass, energy and momentum, see [1] for details and Figure 22 for illustrations. This figure displays the expected values of the energy $\mathbb{E}[\|\nabla u(t)\|^2_{L_2}]$ and of the mass $\mathbb{E}[\|u(t)\|^2_{L_2}]$ along the numerical solutions computed with the stochastic implicit midpoint rule (MP), the backward Euler-Maruyama (BEM), and the stochastic exponential method (SEXP)
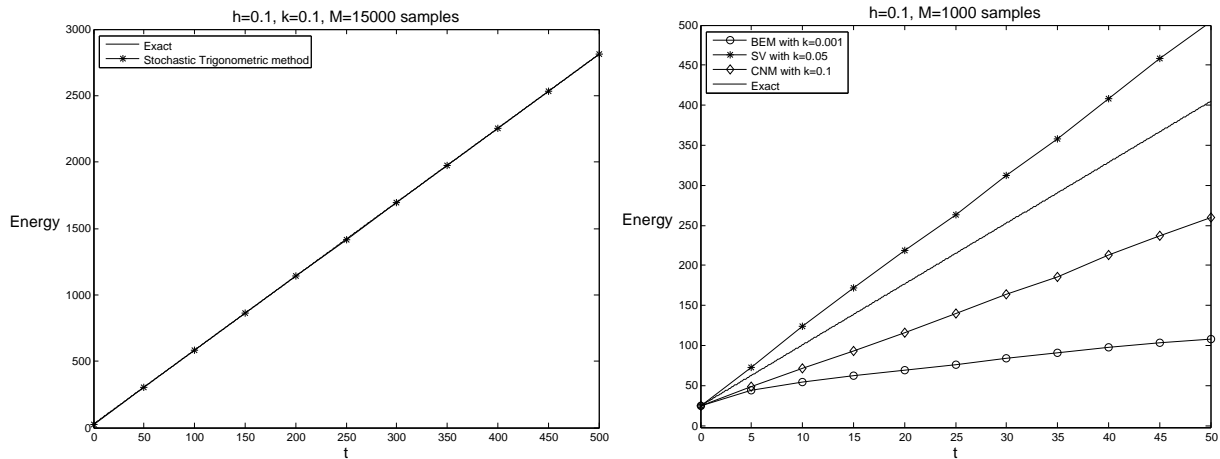
Figure 21: Linear growth in the expected energy of the linear stochastic wave equation for various numerical solutions.
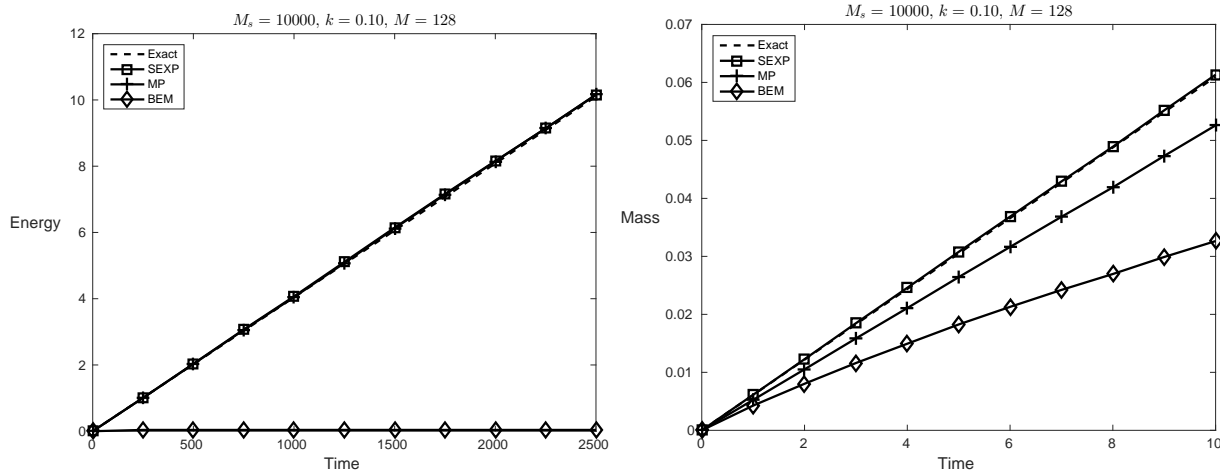


Figure 22: Linear growth in the energy (left) and mass (right) of the linear stochastic Schrödinger equation for various numerical solutions and two different space-time $Q$-Wiener process $W$.

with the time step $k = 0.1$ and $M = 128$ Fourier modes are used for the spatial discretisation. We consider noise of the form

$$W(x, t) = \frac{1}{\sqrt{2\pi}} \sum_{n \in \mathbb{Z}} \lambda_n^{1/2} \beta_n(t) e^{inx} \quad \text{for} \quad 0 \le x \le 2\pi,$$

with i.i.d Brownian motion $\beta_n(t)$. The eigenvalues of the covariance operator $Q$ are given by $\lambda_n = 1/(1 + n^8)$ (smooth noise, first plot) and $\lambda_n = 1/(1 + n^2)$ (less smooth noise, second plot).

# 6   Further examples of GNI and take home message

This is it for this mini-course offering an introduction to GNI. To conclude let us mention further examples of geometric properties of differential equations:

♦ A non-constant function $I(y)$ is called a **first integral** of $\dot{y} = f(y)$ if $I'(y)f(y) = 0$ for all $y$. This implies that every solutions to this differential equation satisfies $I(y(t)) = I(y_0) = \text{Const}$ and $I$ is thus
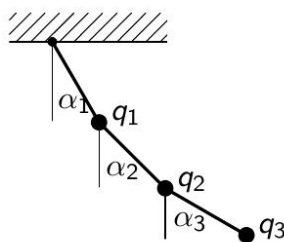
Figure 23: Triple pendulum (courtesy of E. Hairer).

an **invariant**. See the predator-prey problem for example. In this context, one is thus interested in developing numerical methods preserving this invariant.

♦ One can analyse a kind of generalisation of Hamiltonian systems (4), where one allows the matrix $J$ to be non-constant. This is the case for Poisson systems. A **Poisson system** is defined as

$$\dot{y} = B(y)\nabla H(y),$$

where the skew-symmetric matrix $B(y)$ satisfies some properties. The predator-prey problem is an example of a Poisson system. Here, one is interested in developing numerical methods that are Poisson maps. This is more or less the equivalent of symplecticity in this setting. We refer to [12, Chapter VII.2]

♦ **Differential equations on a manifold or differential equation with constraints**. Example: Triple pendulum (see Figure 23). Here, we consider 3 mass points in the plane $q_i \in \mathbb{R}^2$ for $i = 1, 2, 3$. The constraints are given by $\|q_1\|^2 - 1 = 0, \|q_2 - q_1\|^2 - 1 = 0, \|q_3 - q_2\|^2 - 1 = 0$. Here, one is interested in developing numerical methods which stay on the manifold. We refer to [10].

♦ **Composition** and **splitting methods** are powerful techniques to develop high-order geometric numerical integrators. We refer to [3].

♦ Long-time near-conservation of energy and angular momentum for **symmetric multistep methods**.

♦ Symmetry, reversibility, volume preservation, preservation of fixed point, etc.

Finally, I hope that I convince you to

use geometric properties of a (stochastic) differential equation in order to develop efficient numerical methods to solve it!

The following references give an introduction to numerical methods for differential equations (ODE); or offer a good introduction to the subject of this lecture *Geometric Numerical Integration (GNI)* (GNI); or are research articles on (stochastic) GNI (SDE, splitting, exponential integrators). A short comment after some references is also provided.

# References

[1] R. Anton and D. Cohen. Exponential integrators for stochastic Schrödinger equations driven by Ito noise. *Preprint*, 2016.

[2] U. M. Ascher. *Numerical Methods for Evolutionary Differential Equations*, volume 5. Society for Industrial and Applied Mathematics (SIAM), 2008. *Chapters 2 and 6 contain classical material in num. meth. for ODE and GNI.*

[3] S. Blanes and F. Casas. *A Concise Introduction to Numerical Geometric Integration*. CRC Press, Taylor and Francis Group, 25.03.2016. *Introduction on GNI with application to splitting schemes*.

[4] D. Cohen, S. Larsson, and M. Sigg. A trigonometric method for the linear stochastic wave equation. *SIAM J. Numer. Anal.*, 51(1):204–222, 2013.

[5] E. Faou. *Geometric Numerical Integration and Schrödinger Equations*. Zurich Lectures in Advanced Mathematics. European Mathematical Society (EMS), Zürich, 2012. *GNI for PDEs*.

[6] L. Gauckler. *Long-time Analysis of Hamiltonian Partial Differential Equations and their Discretizations*. PhD thesis, Universität Tübingen, 2010. *GNI for PDEs*.

[7] D. F. Griffiths and D. J. Higham. *Numerical Methods for Ordinary Differential Equations*. Springer-Verlag London Ltd., 2010. *Excellent text book on num. meth. for ODE. Contains chapters on GNI*.

[8] E. Hairer. Geometric numerical integration (TU München). `http://www.unige.ch/~hairer/polycop.html`, 2010. *Lecture notes on GNI*.

[9] E. Hairer and M. Hairer. GniCodes - Matlab programs for geometric numerical integration. `http://www.hairer.org/papers/gni.ps`, 2003. *Summary on GNI illustrated with Matlab codes*.

[10] E. Hairer, C. Lubich, and M. Roche. *The Numerical Solution of Differential-Algebraic Systems by Runge-Kutta Methods*, volume 1409 of *Lecture Notes in Mathematics*. Springer-Verlag, Berlin, 1989.

[11] E. Hairer and Ch. Lubich. Numerical solution of ordinary differential equations. `na.uni-tuebingen.de/~lubich/pcam-ode.pdf`, 2012. *Introductory text on num. meth. for ODE*.

[12] E. Hairer, Ch. Lubich, and G. Wanner. *Geometric Numerical Integration*, volume 31. Springer-Verlag, second edition, 2006. *Geometric numerical methods*.

[13] E. Hairer, S.P. Nørsett, and G. Wanner. *Solving Ordinary Differential Equations I. Nonstiff Problems*, volume 8. Springer-Verlag, second edition, 1993. *Advanced book in num. meth. for ODE*.

[14] D. J. Higham. An algorithmic introduction to numerical simulation of stochastic differential equations. *SIAM Rev.*, 43(3):525–546 (electronic), 2001. *Survey article on numerical methods for SDE*.

[15] M. Hochbruck and A. Ostermann. Exponential integrators. *Acta Numer.*, 19:209–286, 2010. *Survey article on exponential methods*.

[16] A. Iserles. *A First Course in the Numerical Analysis of Differential Equations*. Cambridge University Press, second edition, 2009. *Text book on numerical methods for ODE and PDE*.

[17] A. Iserles. Numerical analysis. `http://www.damtp.cam.ac.uk/user/na/NA_papers/NA2012_01.pdf`, 2012. *Introductory text on numerical analysis*.

[18] P. E. Kloeden and E. Platen. *Numerical Solution of Stochastic Differential Equations*, volume 23 of *Applications of Mathematics (New York)*. Springer-Verlag, Berlin, 1992. *Reference book for SDE*.

[19] B. Leimkuhler and S. Reich. *Simulating Hamiltonian Dynamics*, volume 14. Cambridge University Press, 2004. *Geometric numerical methods*.

[20] R. I. McLachlan and G. R. W. Quispel. Splitting methods. *Acta Numer.*, 11:341–434, 2002. *Survey article on splitting methods*.

[21] G. N. Milstein. *Numerical Integration of Stochastic Differential Equations*, volume 313 of *Mathematics and its Applications*. Kluwer Academic Publishers Group, Dordrecht, 1995. *Reference book for SDE*.

[22] G. N. Milstein and M. V. Tretyakov. *Stochastic Numerics for Mathematical Physics*. Scientific Computation. Springer-Verlag, Berlin, 2004. *Reference book for SDE*.

[23] J. M. Sanz-Serna and M. P. Calvo. *Numerical Hamiltonian problems*, volume 7. Chapman and Hall, 1994. *Textbook on GNI*.

[24] A. H. Strømmen Melbø and D. J. Higham. Numerical simulation of a linear stochastic oscillator with additive noise. *Appl. Numer. Math.*, 51(1):89–99, 2004.

[25] E. Süli. Numerical Solution of Ordinary Differential Equations. http://people.maths.ox.ac.uk/suli/nsodes.pdf, 2013. *Lecture notes on num. meth. for ODE*.

[26] E. Süli and D. F. Mayers. *An Introduction to Numerical Analysis*. Cambridge University Press, 2003. *Chapter 12 contains classical material in num. meth. for ODE*.

# 7   Photos and short biographies

For further reading, we refer to http://www-history.mcs.st-and.ac.uk/history/

Leonhard Euler 1707 – 1783 (Basel, Switzerland).
Entered the University at the age of 14. Had Johann Bernoulli as mentor. Worked in almost all areas of mathematics. If all his work would have been printed, this would represent ca. 50 books.
Best mathematician in the world.

Carl David Tolmé Runge 1856 – 1927 (Bremen).
After 6 weeks literature studies, change for math.+physics. Spent some years in Havana, Cuba.
Professors: Max Planck, Weierstrass, Kronecker. Works on differential geometry and numerical analysis. With 70 years old, could still do a handstand.

Martin Wilhelm Kutta 1867 – 1944 (Pitschen, Poland).
Studied math., language, music and art (München). The Runge-Kutta scheme comes from his dissertation. Works on streamlines, glacier and history of math.

John Butcher 1933– (Auckland, New Zealand).
Trees. General linear methods (gen. of RK, multi-step methods).
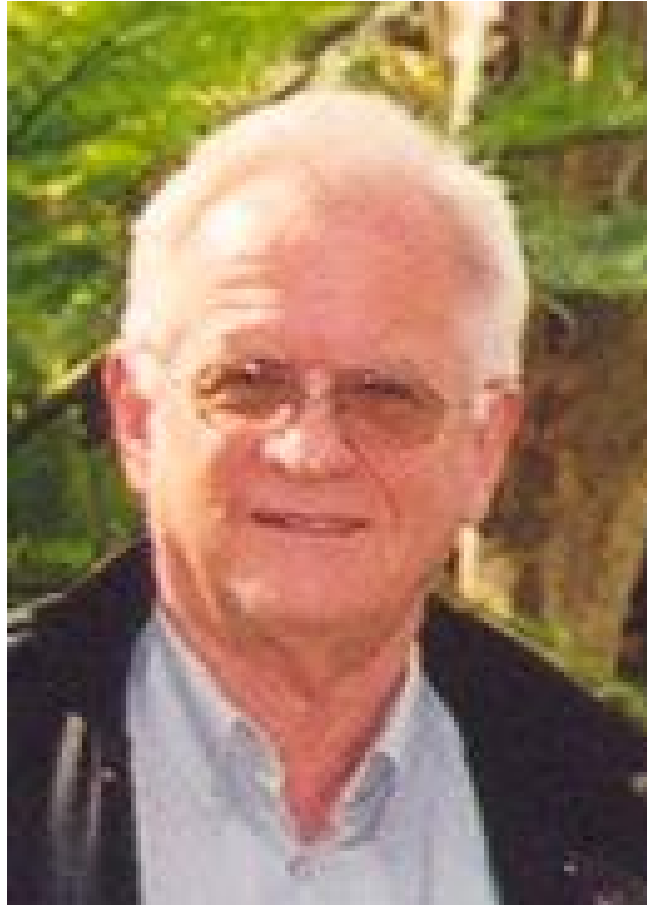
Fredrik Carl Mulertz Störmer 1874 − 1957 (Skien, Norway).
PhD. at the University of Christiana (=Oslo) in 1898. First publication before his PhD. Postdoc in Paris (with Picard, Poincaré, Darboux, Jordan). Prof. at the University of Oslo (1903-1946).
Pictures of Polar light -> numerical scheme.

Loup Verlet 1931– (Paris).
Psychoanalyst and physicist. His numerical scheme was designed in 1967. Afterwards philosopher and writer.

Sir Isaac Newton 1643 – 1727 (Woolsthorpe, Great-Britain).
Trinity College in Cambridge. Studies philosophy and mechanics. Professor in Cambridge with
27 years old. Main work: ODE, integral eq., optics, mechanics, gravitation law, etc. Goes into
politics ($$$$ :-)).

Sir William Rowan Hamilton 1805 – 1865 (Dublin, Ireland).
Speaks Latin, Greek, Hebrew with 5 years old. Reads works from Newton, Laplace (1 error) with 15. Was professor with 22. Main work: mechanics, quaternions, astronomy, etc.

Jules Henri Poincaré 1854 − 1912 (Nancy, France).
Student from Hermite (PhD. on ODE). "Last universalist in mathematics" (math., physics, philosophy). Algebra, algebraic geometry, functional analysis, fluid dynamics, relativity, Poincaré conjecture, etc.

Christian Lubich 1959– (Tirol, Austria).
Geometric numerical integration. General relativity. Quantum and classical molecular dynamics. SIAM Dahlquist Prize.

Ernst Hairer 1949– (Tirol, Austria).
B-series. ODE. Geometric numerical integration. Present in the World record Guinness book
(RK of order 10 with $s = 17$).

Gerhard Wanner 1942– (Tirol, Austria).
B-series. ODE. Geometric numerical integration. Book about the life of Euler.

Enrico Fermi 1901 – 1954 (Rome, Italy).

1918 Scuola Normale Superiore in Pisa. 1923 Göttingen. 1926 Chair of theoretical physics at the University of Rome. 1938 Nobel Prize. Because his wife was Jewish, they had to go to the US (Columbia University). Then worked in Los Alamos (build bomb, works with Pasta, Ulam).
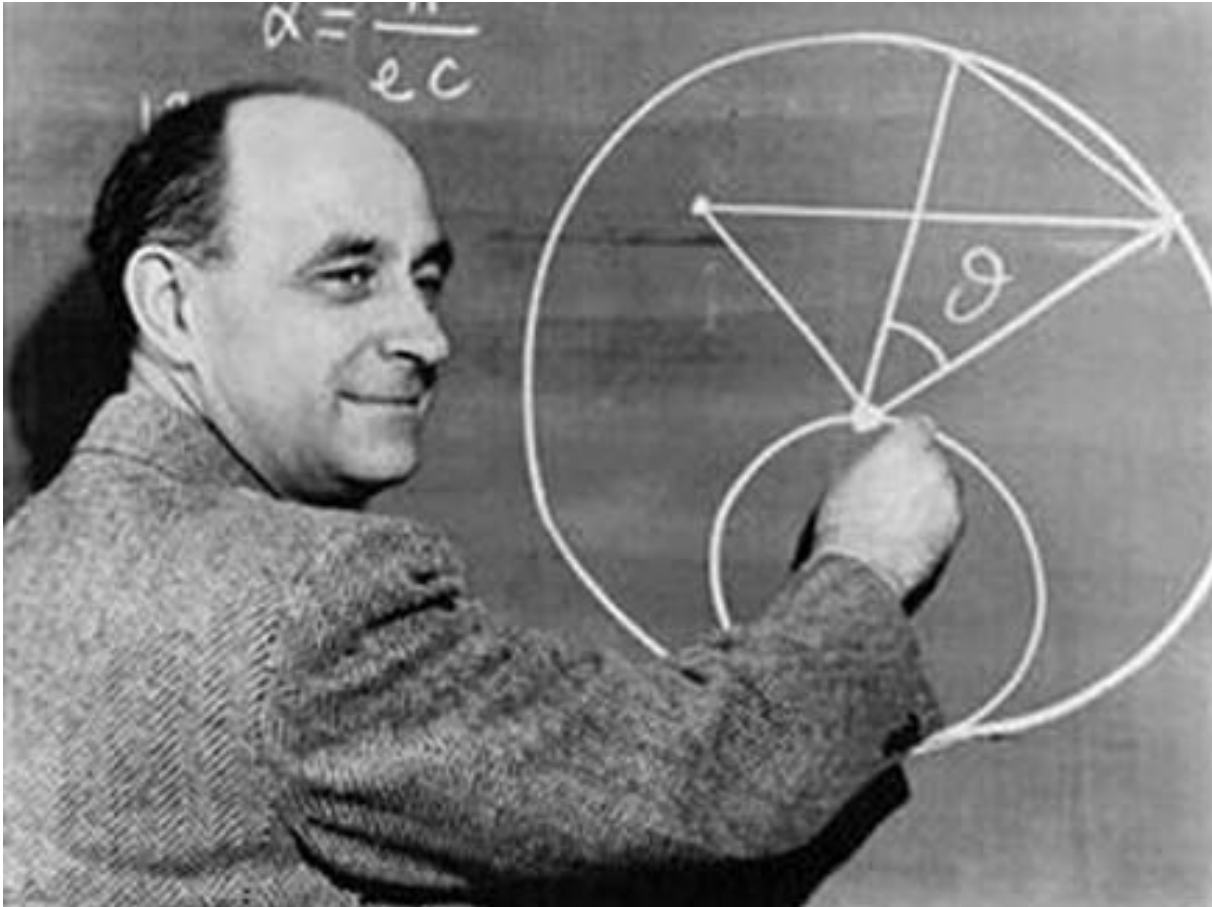
John Pasta 1918 – 1984 (NYC).
Was a New York City police officer from 1941 to 1942. PhD in theoretical physics in 1951 and just after started to work at Los Alamos.
Main projects: Design of a computer specialised in calculations around weapons with Metropolis. FPU problem. Computers.

Stanislaw Marcin Ulam 1909 – 1984 (Lemberg, Poland, Austrian Empire).
1933 PhD under Banach supervision. 1940 Ass. Prof. at the University of Wisconsin. Then worked at Los Alamos (hydrogen bomb).
Main works: Explain how to initiate fusion in the hydrogen bomb. Monte-Carlo method (finance, probability, sampling). Set theory. Measure theory. Ergodic theory. Group theory. Topology. Mathematical physics.